Elastic parameters characterization of multilayered structures by air-coupled ultrasonic transmission and genetic algorithm

Victor Takahashi, Michaël Lematre, Jérôme Fortineau, Marc Lethiecq

Elastic Parameters Characterization of Multilayered Structures by Air-Coupled Ultrasonic Transmission and Genetic Algorithm

Victor Takahashi, Michaël Lematre,
Jérôme Fortineau, Marc Lethiecq¶ [1]

GREMAN UMR 7347, Université de Tours, INSA Centre Val de Loire, CNRS, 3 Rue de la Chocolaterie, Blois, France

***Abstract*—** This paper describes a non-contact method to characterize isotropic and anisotropic planar multilayer structures using a genetic algorithm. The method is based on the determination of critical angles, where the maxima of the modulus of transmission coefficient of the structure appear, and which correspond to the generation of guided waves. The optimization process minimizes the error between the reference critical angles and associated amplitudes of the transmission coefficient, with the corresponding estimated ones. The estimation of elastic parameters is demonstrated for acrylic and oak plates as well as for a bi-layered structure composed of oak and a thin layer of gesso. It is shown that to obtain satisfactory optimization results, it is necessary for guided modes of higher order than the zero ones to be taken into account. Results also show that some elastic constants such as C_{33} and C_{55} retrieved from the transmission coefficient are very sensitive to the optimization.

Keywords - guided waves, transmission coefficient, critical angles, genetic algorithm, optimization, isotropic and anisotropic structures

1. Introduction

The monitoring of structures and material characterization by nondestructive techniques has become widespread in automotive, aerospace, infrastructure construction and other industries. These techniques provide information about the condition and possible flaws, even for complex structures such as composites and multilayers. Thermograghy, X-rays, ultrasonic waves, are some of the most common NDE methods applied in industry to analyze materials [1]. Ultrasonic techniques are particularly used to characterize elastic properties of materials because acoustic wave properties such as velocity and attenuation are directly linked to the material characteristics [2]. Such characterizations generally require a coupling medium between transducers and sample, which can be water-based gel, oil or glue (for contact measurements) or water (for immersion measurements). Classical transducers do not allow using air as a coupling medium due to the huge impedance mismatch. In some applications, the use of these coupling media is not feasible e.g. the characterization of cultural heritage paintings or of samples that react in contact with liquids [3], [4], [5], [6], [7]. Progress in air-coupled transducers in the last few years allows their use

for non-contact nondestructive inspections in research and industrial context [8], and has been considered for the inspection of artwork, in combination with a thermal technique [9]. For example, Hosten et al. [10] characterized an anisotropic material using bulk wave phase velocity measurements. However, only thick samples have been tested, because multi-path transmission signals overlap and cannot be separated in time. Castaings et al. in [11] used air-coupled ultrasonic transducers to estimate the elastic constants in of isotropic and anisotropic materials based on transmission field and numerical model using the Thomson-Haskell matrix method. Despite giving coherent results, the method implies long computational times since the inverse process uses a combination of Simplex and Newton–Raphson methods. Elastic constants of anisotropic and orthotropic materials were retrieved, by Hosten et al. in [12] and Dahmen et al. in [13], respectively, in a single side plate configuration, through a phase velocity measurement and minimization process based on a hybridization of Newton–Raphson and Simplex methods. The phase velocity was measured through 2D Fourier Transform of signals obtained by varying the distance between the transmit and receive (Tx & Rx) transducers in small steps. Zhang and Chimenti showed that the transmission coefficient could be reconstructed using the spectral sum of frequency and spatial signals [14]. They acquired transmitted signals by varying the incident angle and distance between transducers, on isotropic and anisotropic materials. The elastic constants are then estimated with a Simplex inversion process of the experimental transmission coefficient and a 3D transducer model. Considering a 3D representation of the wave produced by the transducer, results show a slight change compared to the hypothesis of a plane incident wave, with small variation in the imaginary part of the complex elastic constant, which corresponds to the attenuation of the wave inside the material.

This paper presents a procedure to characterize isotropic and anisotropic materials by estimating their elastic constants and mass density, through an optimization procedure based on the use of a Genetic Algorithm (GA) applied on the modulus of the transmission coefficient for varying incidence angles.

The transmission coefficient is computed based on the stiffness matrix method by Rokhlin and Wang in [15]. This method was adopted since it has higher stability, when the frequency-thickness product increases (roughly higher than 20 MHz.mm), compared to the classical transfer matrix one. This will be the case, especially when thick layers of wood will be studied in regard to wavelengths in our frequency range. Our optimization process is based on a Genetic Algorithm (GA), whose capability to estimate elastic constants has proved highly efficient in the last few years [16] [17] [18] [19]. The capacity to find solutions in non-smooth and non-continuous objective functions and also the possibility to use large individuals' boundaries, turns GA into a powerful optimization tool to estimate elastics constants. Furthermore, the process of minimization using GA can be easily parallelizable, decreasing the computational time to find the optimal solution. This work aims to show numerically the capability of a Genetic Algorithm to retrieve the elastic parameters of a sample, when using only critical angles and corresponding amplitude of the peaks that appear in the modulus of the transmission coefficient versus incidence angle, instead of using the whole of this coefficient. It allows to gain computation time and to highlight the fact that

these specific regions of the transmission coefficient are sufficient to determine the elastic properties of the sample.

Experimental data used here is taken from the literature and references are given in the text. Furthermore, in an experimental analysis, this method would avoid the need for a calibration of the transducers in transmission mode.

The transmission coefficient is computed both to simulate a measured one with targeted elastic parameters values, and to simulate the one with optimized elastic parameters. Section 2 briefly describes the theory to calculate the transmission coefficient with the recursive matrix method and defines the objective function to be minimized. Section 3 defines the parameters of the inverse problem and presents the computation steps proposed to retrieve the material properties. Section 4 presents the simulation results, showing the capability of the method to retrieve elastic parameters for different types of materials. First, a plate of isotropic acrylic is studied, with two independent elastic constants. Then, the mass density of the same acrylic plate with independent elastic constants, is considered as unknown parameter. The method is also applied using Simplex as optimization algorithm for sake of comparison. Finally, a simulated orthotropic material based on oak properties and a double layer consisting of a thin layer of gesso coated on a thick oak layer, are studied. Gesso is an element of old panel paintings, also known as ground layer. It was traditionally composed of rabbit-skin glue and ground chalk, allowing a smooth paintable surface on wood panels. This is a typical structure of heritage paintings for which it is difficult to determine the elastic properties and density. Indeed, since the common practice involves hand manipulation and contact methods, such measurements could damage the structure and paintings. Therefore, the use of a sample surrounded by air for this application is a technical alternative to mechanically evaluate and characterize the artwork.

2. Forward problem

The principle of our method is sketched in Fig. 1. An ultrasonic longitudinal wave, assumed to be a plane wave, is generated in air by a transmitting transducer and a receiving transducer is placed on the other side of the sample. The sample can be turned by an angle θ_i along the X_2 axis, while the two transducers operating in through-transmission mode are fixed. Concerning the sample surface, the angle θ_i thus corresponds to the incident angle of the longitudinal wave emitted by the transmitter. The incident wave then propagates through the entire thickness d of the plate and can be partly converted into transverse waves. Depending on the angle θ_i, the longitudinal and transverse waves can combine to give guided waves that radiate a part of their energy into the air. These transmitted waves are received on the opposite side of the sample with the same angle θ_i. For a specific frequency the transmission coefficient is calculated as a function of the incidence angle θ_i.

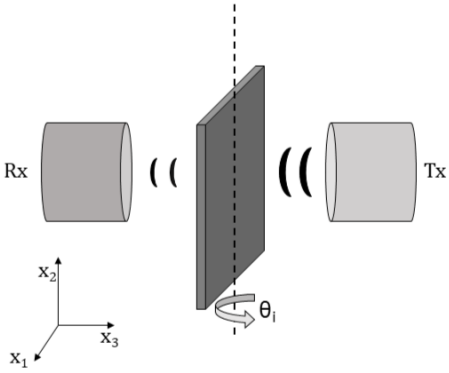

Fig. 1. Air-coupled through-transmission system.

The transmission coefficient is computed based on the stiffness matrix method described by Rokhlin and Wang [15]. This method has the advantage of having higher numerical stability than the Thomson-Haskell method that was used for example in [11] and [12], mainly when the frequency-thickness product increases. The stiffness method considers three displacement and stress vectors on the top face of each layer and three displacement and stress vectors on its bottom face. Hence, a recursive matrix operation computes the global matrix, instead of the inverse matrix multiplication that is implemented in the transfer matrix method, and which is unstable for high frequency-thickness products due to exponential matrix operations. The calculation of the transmission coefficient through this method can be summarized as follows:

Considering a displacement vector u_m and stress vector σ_m for a mth layer.

$$u_m = \sum_{j=1}^{3} \left[a_j^+ p_j^+ e^{ik_z^{+j}(z-z_m)} + a_j^- p_j^- e^{ik_z^{-j}(z-z_{m-1})} \right]^m \times e^{i(k_x x + k_y y - \omega t)} \quad (1)$$

$$\sigma_m = \sum_{j=1}^{3} \left[a_j^+ d_j^+ e^{ik_z^{+j}(z-z_m)} + a_j^- d_j^- e^{ik_z^{-j}(z-z_{m-1})} \right]^m \times e^{i(k_x x + k_y y - \omega t)} \quad (2)$$

where the displacement vector u_m possesses the components (u_1^m, u_2^m, u_3^m) and the stress vector σ_m possesses the components $(\sigma_{31}, \sigma_{32}, \sigma_{33})$. The components of the stress vector, σ_{3j} (j=1,2,3), correspond to components that are applied on a surface possessing a

normal along the (z) axis where a_j^{+-} are the wave amplitudes, p_j^{+-} is the displacement polarization vector, d_j^{+-} is the stress polarization vector, k_z^{-+j} are the wavenumbers in $-z$ and $+z$ directions, respectively, z_m and z_{m-1} are the local coordinates of each layer, where $(z = z_{m-1})$ for the waves propagating in the $-z$ direction and $(z = z_m)$ for waves propagating in the $+z$ direction, ω is the angular frequency and t the time.

Considering the submatrices P^+=[p_1^+,p_2^+,p_3^+], P^-=[p_1^-,p_2^-,p_3^-], D^+=[d_1^+,d_2^+,d_3^+], D^-=[d_1^-,d_2^-,d_3^-] and H^+=Diag[$e^{ik_z^{+1}h_m}$,$e^{ik_z^{+2}h_m}$,$e^{ik_z^{+3}h_m}$], H^-=Diag[$e^{-ik_z^{-1}h_m}$,$e^{-ik_z^{-2}h_m}$,$e^{-ik_z^{-3}h_m}$], and h_m= $z_{m-1} - z_m$ being the thickness of the mth layer, Eq. (1) and Eq. (2) can be written in a matrix form of Eq. (3) and Eq. (4):

$$\begin{pmatrix}\sigma_{m-1}\\ \sigma_m\end{pmatrix} = \begin{bmatrix}D^- & D^+H^+\\ D^-H^- & D^+\end{bmatrix}\begin{pmatrix}A_m^-\\ A_m^+\end{pmatrix} \tag{3}$$

$$\begin{pmatrix}u_{m-1}\\ u_m\end{pmatrix} = \begin{bmatrix}P^- & P^+H^+\\ P^-H^- & P^+\end{bmatrix}\begin{pmatrix}A_m^-\\ A_m^+\end{pmatrix} \tag{4}$$

The stiffness matrix K^m of the m-th layer is then calculated substituting the amplitudes of Eq. (3) in Eq. (4), as a result this is a (6×6) matrix written as:

$$K^m = \begin{bmatrix}D^- & D^+H^+\\ D^-H^- & D^+\end{bmatrix}\begin{bmatrix}P^- & P^+H^+\\ P^-H^- & P^+\end{bmatrix}^{-1} \tag{5}$$

The stiffness matrix of the layered media can be obtained by combining the stiffness matrix of each layer in a recursive calculation. For example, in the case of a bi-layered structure with the first stiffness matrix K^1 and the second stiffness matrix K^2, the total stiffness matrix Eq.(8) is computed by relating σ_0 and u_0 to σ_2 and u_2 and suppressing σ_1 and u_1 from Eqs.(6) and (7):

$$\begin{pmatrix}\sigma_0\\ \sigma_1\end{pmatrix} = \begin{bmatrix}K_{11}^1 & K_{12}^1\\ K_{21}^1 & K_{22}^1\end{bmatrix}\begin{pmatrix}u_0\\ u_1\end{pmatrix} \tag{6}$$

$$\begin{pmatrix}\sigma_1\\ \sigma_2\end{pmatrix} = \begin{bmatrix}K_{11}^2 & K_{12}^2\\ K_{21}^2 & K_{22}^2\end{bmatrix}\begin{pmatrix}u_1\\ u_2\end{pmatrix} \tag{7}$$

$$\begin{pmatrix}\sigma_0\\ \sigma_2\end{pmatrix}=\begin{bmatrix}K_{11}^1+K_{12}^1(K_{11}^2-K_{22}^1)^{-1}K_{21}^1 & K_{12}^1(K_{11}^2-K_{22}^1)^{-1}K_{12}^2\\ K_{21}^2(K_{11}^2-K_{22}^1)^{-1}K_{21}^1 & K_{22}^2+K_{21}^2(K_{11}^2-K_{22}^1)^{-1}K_{12}^2\end{bmatrix}\begin{pmatrix}u_0\\ u_2\end{pmatrix} \quad (8)$$

Generalizing this method to a multilayered structure of M layers, the global stiffness matrix is obtained recursively using Eq. (8):

$$K^M=\begin{bmatrix}K_{11}^{M-1}+K_{12}^{M-1}(K_{11}^m-K_{22}^{M-1})^{-1}K_{21}^{M-1} & K_{12}^{M-1}(K_{11}^m-K_{22}^{M-1})^{-1}K_{12}^m\\ K_{21}^m(K_{11}^m-K_{22}^{M-1})^{-1}K_{21}^{M-1} & K_{22}^m+K_{21}^m(K_{11}^m-K_{22}^{M-1})^{-1}K_{12}^m\end{bmatrix} \quad (9)$$

where K^M is the total stiffness matrix for the top m layers, K_{ij}^{M-1} is the total stiffness matrix for the top $m-1$ layers, and K_{ij}^m are the stiffness matrix elements for the mth layer. Fig. 2 shows a multilayer structure, consisting of N arbitrary anisotropic layers.

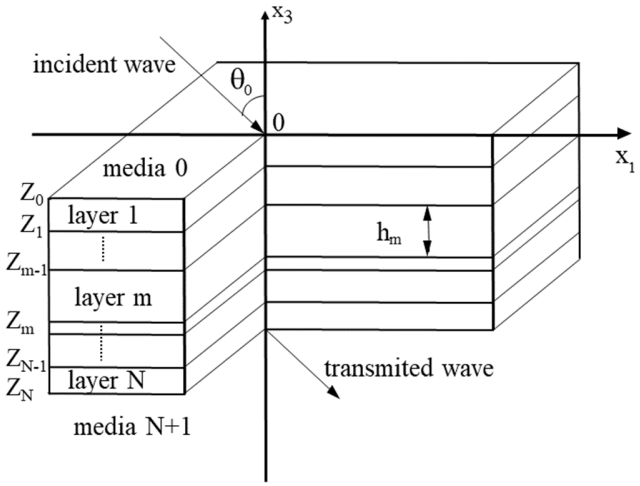

Fig. 2. Multilayer structure

Following the procedure described by Rokhlin and Wang in [15], the transmission coefficient in air, in which only longitudinal waves propagate, is therefore obtained when the upper and bottom shear stresses are set to zero. Relating the normal displacement and stress of the last layer with the transmission field into the coupling fluid, the equation which describes the transmission coefficient is written as:

$$T=\frac{2\Omega S_{21}^{33}}{(S_{11}^{33}+\Omega)((S_{22}^{33}-\Omega)-(S_{21}^{33}S_{12}^{33})} \quad (10)$$

where S=K^{-1} is the compliance matrix calculated from the inverse of the global stiffness matrix, S_{ij}^{33} are the (3,3) elements of each sub-matrix of the compliance matrix S and Ω is defined as:

$$\Omega = \frac{cos\theta_i}{i\omega\rho_f V_f} \tag{11}$$

where ρ_f and V_f are the mass density and speed of sound of air.

For a given frequency, the modulus of the transmission coefficient has a pattern with different peaks as a function of the incidence angle θ_i. When the impedance of the multilayer structure is much higher than the one of the surrounding media, the peak locations coincide with the critical angles that form Lamb modes inside the medium. Brekhovskikh and Godin have named this the "coincidence rule" in [20] . Since these critical angles are function of the values of the elastic constants C_{ij}, mass density ρ, and thickness d, they will be used specifically for the inverse problem in order to retrieve these elastic parameters.

3. Inverse problem

From the transmission coefficient computed for a given sample as indicated in the previous section, the material parameters will be estimated by a minimization process. The function to be minimized is an error function which compares the modulus of a simulated transmission coefficient taken as a reference, with the modulus of a transmission coefficient that is computed with the set of guessed parameters generated by an optimization algorithm. The simulated transmission coefficient that will serve as reference, named T_r, is computed with the known property values of the material, C_{ij}, ρ and d as described in section 2, and its critical angles and corresponding peaks are compared with those of the transmission coefficient, named T_o, which is generated at each step of the optimization process. Thus, the objective function to be minimized is formulated by comparing the peak amplitudes $[A_r, A_o]$ and the corresponding critical angles $[\theta_r, \theta_o]$ of the transmission coefficient modulus T_r with those of T_o.

Hence, the objective function is defined as:

$$F(C_{ij}) = \sum[\sum(\theta_r - \theta_o)^2 + \sum(\mathrm{A}_r - \mathrm{A}_o)^2] \tag{12}$$

where A_r and A_o are the amplitudes of the peaks corresponding to the critical angles $[\theta_r,\theta_o]$.

The estimation of the elastic constants is obtained by an optimization process using a Genetic Algorithm (GA), an algorithm based on Darwin's theory of evolution. The population (solution) randomly changes slightly and slowly in each generation converging to a best solution. Preliminary trials of elastic parameters optimization with the GA reveals that when the constraints have unknown parameters (individuals) that are comprised in a wide range of values, and far away from the expected ones, different combinations of elastic constants C_{ij}, minimize the objective function with the same peak locations in the transmission coefficient, whatever the frequency. However, depending on the elastic constants found by

solving the inverse problem, the multiple peaks differ in amplitude, making the information of amplitude crucial to estimate the right solution.

One of the limitations of GA is the fact that the solution sometimes cannot converge to the minimum global point, and instead, can be trapped in a local minimum. A non-uniform mutation decreases the chances of this occurrence. However, since large boundaries are applied - and GA is a stochastic model - it does not guarantee convergence to the global minimum, but an approximation of it. In order to extract and perform statistical analysis of the results, the GA runs twenty times each optimization for each material, giving stochastic information about results (mean and standard deviation) as sketched in the organizational chart of Fig. 3.

The GA is based on elitism selection, in which the best individuals are automatically selected for the new generation without any modification, and a roulette selection of "parents" for the next generation based on stochastic simulation. The crossover fraction is defined to be 0.8 which means that 80% of the "children" from next generation are built through crossover operation and the other 20% generated through mutation operation. The mutation function chooses a mutation rate for each individual in the parent vector, following a Gaussian distribution. The mutation function parameters force a higher mutation rate in the first generations, which decreases to 0 in the final step, while the total number of generations is fixed at 200. These parameters were pre-tuned with different combinations to give good results in the inversion process for the same objective function. Once the parameters were found, they were kept constant for the following different cases. The tests were performed by using a computer based on an Intel® core i7 processor 8th gen., with 16 GB of RAM.

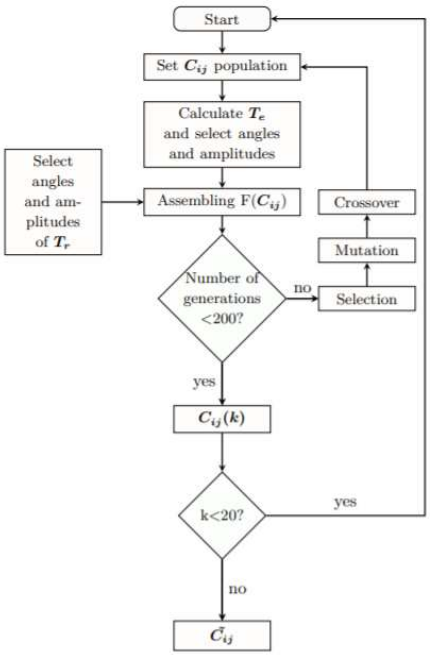

Fig. 3. GA Flowchart

4. Elastic constants estimation results

In order to demonstrate the capability of our backward method that uses a GA optimization process applied in a certain angular range of the transmission coefficient, we will present the optimization results on samples of different types and symmetries. The transmission coefficient is computed based on Eq. (10) , that allows to simulate a viscoelastic and homogeneous medium surrounded by air of plane wave velocity v_{air} = 343 m/s and mass density ρ_{air} = 1.22 kg/m^3. The incident angle has a range from 0° to 60°, that allows to visualize all the guided modes appearing in the different samples.

4.1. Acrylic Plate Sample

The first analyzed sample is an isotropic 3mm thick acrylic plate with a mass density of 1200 kg/m^3. The reference transmission coefficient T_r is generated with the set of elastic constants and mass density measured by Dodd et al. in [21]. Since the sample is isotropic, it possesses only two independent elastic constants, C_{11} and C_{13}, where C_{55} follows the relationship

$$C_{55} = (C_{11} - C_{13})/2 \tag{13}$$

The elastic constant matrix of this acrylic plate is thus defined as:

$$[C_{ij}] = \begin{bmatrix} 8.6 & 4.4 & 4.4 & 0 & 0 & 0 \\ 4.4 & 8.6 & 4.4 & 0 & 0 & 0 \\ 4.4 & 4.4 & 8.6 & 0 & 0 & 0 \\ 0 & 0 & 0 & 2.1 & 0 & 0 \\ 0 & 0 & 0 & 0 & 2.1 & 0 \\ 0 & 0 & 0 & 0 & 0 & 2.1 \end{bmatrix} [GPa]$$

The critical angles and their associated amplitudes that appear in the modulus of T_r are compared with the corresponding ones of T_o created at each GA generation. The lower and upper boundaries of the population chosen for this simulation are 5 GPa and 15 GPa for C_{11} and 2 GPa and 7 GPa for C_{13}.

4.1.1. Characterization of elastic parameters at 200 kHz

In a first trial to characterize the elastic constants, a frequency of 200 kHz is chosen to generate the transmission coefficient, whose modulus is represented in Fig. 4. The estimated transmission coefficient is calculated using the mean elastic parameters, given in Table 1. In Fig. 4 one can observe two peaks located at the critical angles using the reference and two other peaks using the mean values of estimated elastic constant. These peaks correspond to the zero-order Lamb modes A0 and S0. The shift in the incident angles is quite significant, due to unsatisfactory optimization.

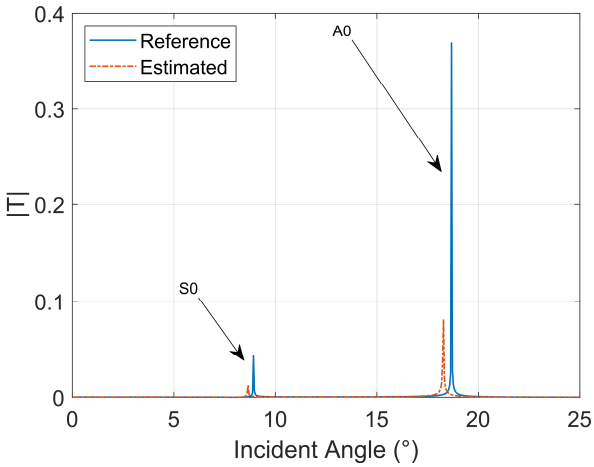

Fig. 4. Comparison between transmission coefficients for reference and estimated acrylic plate constants at 200 kHz .

	N°of modes	C_{11}(GPa)	C_{13}(GPa)	C_{55}(GPa)
Reference 1 MHz	8	8.6	4.4	2.1
Estimated 200kHz	2	8.32±1.53	3.81±1.92	-
Estimated 1 MHz	6	8.61±0.09	4.40±0.09	2.08±0.01

Table 1 Estimated parameters of acrylic, mean value standard deviation after twenty rounds of optimization

With such a difference in the mean values and a high value of standard deviation of C_{13} and C_{11}, the estimation cannot be considered as satisfactory. Indeed, the results have shown that other individuals can minimize the objective function with a transmission coefficient that contains the same critical angle locations and very close amplitudes. However, increasing the frequency to 1MHz allows to excite more modes, of higher order, as illustrated in Fig. 5. Hence, with more peaks in the transmission coefficient, the GA has better chance to find the global minimum of the objective function.

4.1.2. Characterization of elastic parameters at 1 MHz

For this frequency value of 1 MHz, it was found that the values of C_{11} and C_{13} were correctly retrieved, for the same lower and upper boundaries of the population parameters. Then, even if the sample is isotropic, the elastic constant C_{55} was considered as an unknown parameter in the inversion problem, in order to evaluate the robustness of the optimization method and verify that the equality Eq. (13) remains valid. The boundaries of C_{55} were set between 1 GPa and 3 GPa. Table 1 shows the three estimated parameters at 1 MHz.

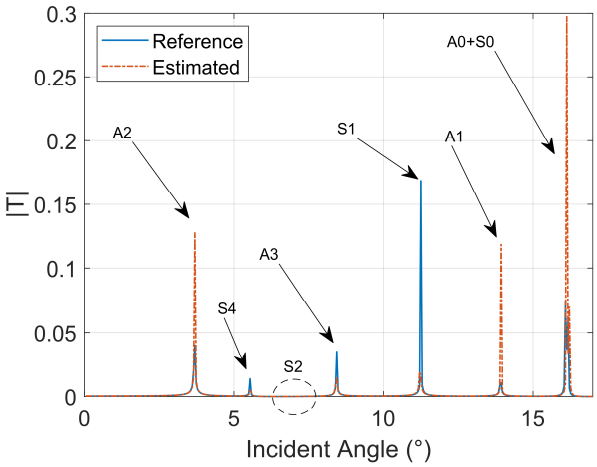

Fig. 5. Comparison between transmission coefficient of reference and estimation for 3mm acrylic plate at 1MHz. Dashed circle shows the location of a mode with very small transmission

It is possible to see in Fig. 5 that the transmission coefficient contains six peaks, both for the reference and estimated values. However, a small peak that represents the symmetric mode S2, whose location is marked by the dashed circle in Fig. 5 is also present in the transmission coefficient. It was not taken into account in the computation since its peak amplitude would be too small to be observable. The modes A0 and S0 are combined in a single peak, due to their proximity. Therefore, at 1MHz, the acrylic plate has eight modes as can be seen in the dispersion curve of Fig. 6. The dispersion curves are here represented as a function of the incidence angle, instead of phase velocity, over frequency. Indeed, one can obtain the incident angle according to $\theta_i = sin^{-1}(\frac{v_{air}}{v_{phase}})$. The six observable peaks are used with their associated angle and amplitude values for computation in the optimization process. Table 1 also shows the results for the case where the acrylic plate is exposed to higher frequency, which allows to have better estimated values of the elastic parameters. The standard deviation also helps to evaluate the quality of the optimization and increasing the number of peaks in the transmission coefficient also allows to considerably decrease the standard deviation. The dependent elastic constant C_{55} has a value of 2.08 GPa $\pm$ 0.01 proving that the algorithm is robust since the isotropic mathematical relationship Eq. (13) can be verified for the optimized value of C_{55} that was considered as an independent parameter.

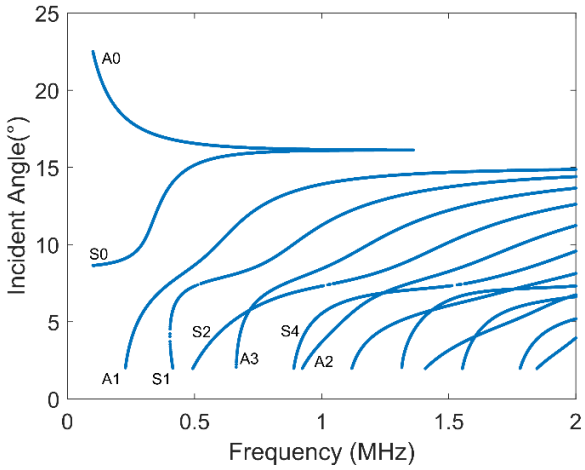

Fig. 6. Dispersion curve of 3 mm acrylic plate with eight modes generated at 1MHz.

In order to further evaluate the robustness of our method, it is then tested with one more parameter to be obtained. The mass density is now also considered as an unknown parameter whose values are very different from those of elastic constants. With four unknown parameters to be retrieved, the algorithm is more susceptible to find other combinations that also minimize the objective function instead of the reference values. The bottom and upper mass density boundaries used in the optimization are 1000 and 1400 kg/m^3, respectively. The results of the mean values and standard deviation are shown in Table 2. The elastic constants standard deviations are roughly 8 times, 4 times and 10 times higher for C_{11}, C_{13} and C_{55}, respectively, compared to values from Table 1 this result shows that, for different trials, the G.A. finds other parameters near the reference ones, that minimize the objective function, but the mean values are still very close to the reference ones. Fig. 7 shows the good agreement between the reference and fitted angles of the transmission coefficient when using the corresponding reference and mean estimated parameters, respectively.

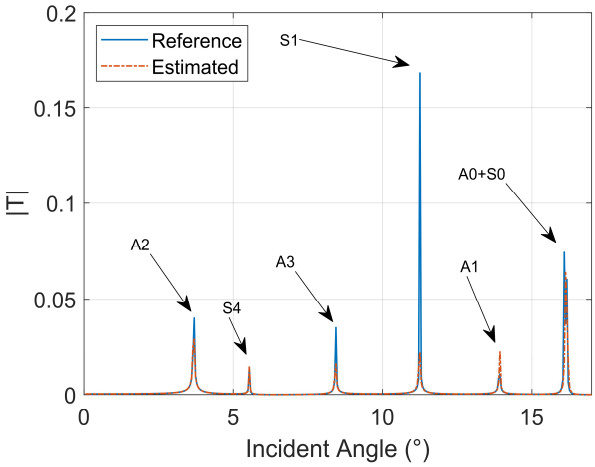

Fig. 7. Transmission coefficient of 3mm acrylic plate at 1MHz with elastic constants and mass density as unknown parameters.

	C_{11}(GPa)	C_{13}(GPa)	C_{55}(GPa)	ρ(kg/m^3)
Reference	8.6	4.4	2.1	1200
Estimated	8.58 ± 0.75	4.39 ± 0.41	2.08 ± 0.17	1194.8 ± 100

Table 2 Elastic constants and mass density estimated for acrylic at 1MHz.

4.1.3. Comparison of optimization performance between of the GA and the Simplex methods

In this section we will compare two methods of optimization: the GA and the Simplex. The simplex algorithm is a typical method of optimization that has been used to find elastic constants of material using ultrasound [22]. A variation of the classical Simplex, that does not use numerical gradients, known as the "Nelder-Mead (NM) Simplex" [23] is adopted to compare with GA. This method is suitable for any type of objective function, i.e. linear or not, with or without discontinuities, and therefore proper to compare with the GA. The NM method does not use constraints and the optimization starts by an initial vector with the size of the variable to be estimated. The estimated values using the NM method are computed starting from different initial guesses of elastic constant values to test the capacity to retrieve those of the previously studied acrylic sample. Only the two independent elastic constants are considered as the input of the optimization. The initial values were chosen by considering a polar coordinate where the x-axis is the parameter C_{11} and y-axis the parameter C_{13}. The radius is fixed to 1GPa with the angles varying from 0 to 2π by steps of $\pi/32$ and the origin at the target values of C_{11} and C_{13}.

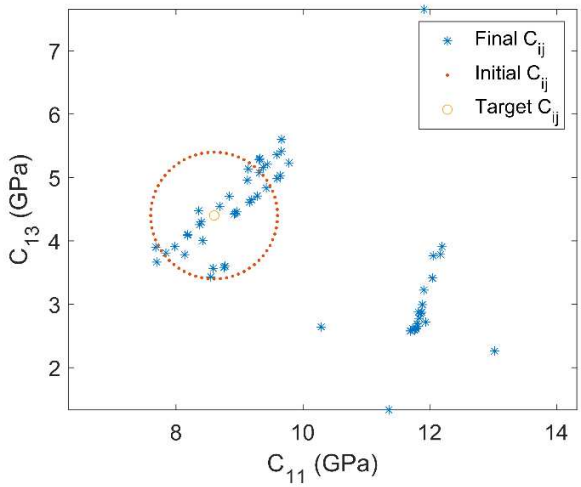

Fig. 8. Optimization of acrylic plate elastic constants by the NM Simplex method.

Fig. 8 shows the initial values marked by a dot (°) and the final values (after optimization) marked by an asterisk (*) of elastic constants C_{11} and C_{13}. The optimization is found to be very dispersive for many initial guess values, with few final values that reach the neighborhood of the target one. This result allows to conclude that the GA is more efficient and robust than the NM Simplex method to find the right estimated parameters, mainly when the initial guess is far from the target value or when the target value is completely unknown. However, if time-consumption is crucial and the initial guess is near the target one, the NM Simplex can be an alternative since it is faster than GA, where at least an hour is required to reach a solution.

4.2. Oak wood

The method is not limited to isotropic samples. In order to study a material with four independent elastic parameters, an oak wood sample is now considered. The sample thickness is 3mm with a mass density of 670 kg/m^3 and elastic parameters defined by Kumar in [24] as:

$$[C_{ij}] = \begin{bmatrix} 14.3 & 0.8 & 1.5 & 0 & 0 & 0 \\ 0.8 & 1.0 & 1.0 & 0 & 0 & 0 \\ 1.5 & 1.0 & 2.1 & 0 & 0 & 0 \\ 0 & 0 & 0 & 0.3 & 0 & 0 \\ 0 & 0 & 0 & 0 & 0.7 & 0 \\ 0 & 0 & 0 & 0 & 0 & 0.8 \end{bmatrix} [GPa]$$

The analyzed plane of symmetry is the 1-3 plane that is parallel to the fibers of the wood, which has four independent elastic constants. Optimization results for oak reveals that the size of the population must be increased to 300 individuals to have satisfactory results. This can be explained by the range of elastic constant boundaries, comprised between roughly 0 and 20 GPa, which is applied to each elastic constant, and by the fact that orthotropic materials have elastic constant values with high deviation between them. Table 3 shows the results of the estimation for the oak sample. Despite the standard deviation of C_{11} and C_{13} of around 10 %, the estimated values are convincing, showing that GA can find

parameters that approach the global minimum. One can also note that in an orthotropic sample, the optimization is more sensitive to elastic constants C_{33} and C_{55}: the optimization can better retrieve the values of these two parameters than those of C_{11} and C_{13}. Furthermore, it was verified that a second round of optimization using an initial population based on the results of the first round gives better results.

	C_{11}(GPa)	C_{33}(GPa)	C_{13}(GPa)	C_{55}(GPa)
Reference	14.3	2.1	1.5	0.7
Estimated	14.4±1.3	2.1±0.07	1.4±0.3	0.7±0.003

Table 3 Elastic constants estimated for oak (plane 1-3)

Fig. 9 shows the transmission coefficient using the mean estimated values and the reference one. It is not possible to see all the modes that can be generated in the sample in Fig. 9 since some have very small transmission amplitudes. However, the "hidden" modes, S3 and A3, can be seen on the dispersion curve in Fig. 10. Since these two modes have very small amplitudes, they were not computed in the optimization process. Thus, the optimization process can estimate the parameters even without using all the modes for a given sample when an orthotropic sample is considered.

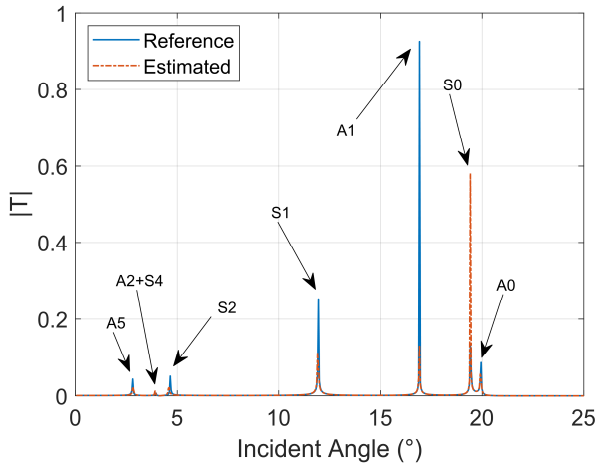

Fig. 9. Comparison between transmission coefficient of reference and estimaion for oak at 1MHz.

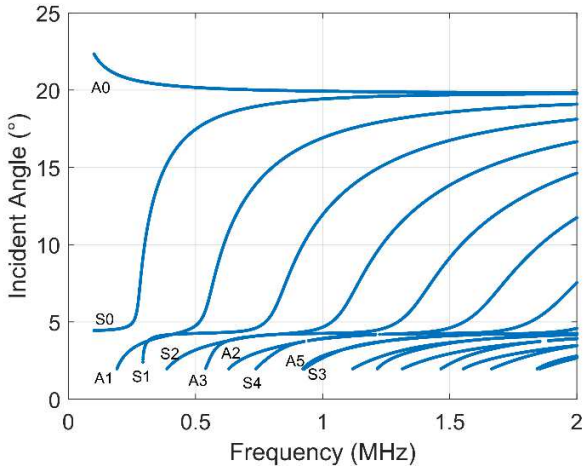

Fig. 10. Dispersion curve of a 3 mm oak plate, showing the different modes excited at 1MHz.

4.3. Oak-gesso two layer structure

Our method is now applied to a bi-layer medium consisting of a thin layer of gesso laid on a thick layer of oak. Gesso can be considered as an isotropic material with Young's modulus E = 3.6 GPa and poisson ratio ν = 0.2, which gives C_{11}, C_{55} and C_{13} equal to 4 GPa, 1.5 GPa and 1 GPa, respectively. The density varies from 500 to 800 kg/m^3 [25] and [26]. In old paintings, mainly from the renaissance epoch, the panels had a thickness in the range roughly from 2 to 15 mm. Following this consideration, a 10 mm panel made of oak oriented in 1-3 plane is chosen to be the support while a gesso layer with a thickness of 132 μm is deposited to obtain a two-layer structure. Two different optimization configurations are considered for this structure. In the first case, the two independent elastic constants of gesso as well as the third elastic constant were the parameters to be retrieved by the minimization process. In the second case, the density of gesso is also supposed unknown and a value to be estimated through the optimization. Fig. 11 shows the transmission coefficient of a single 10mm thick layer of oak superimposed with the one corresponding to the two-layer structure formed with the addition of the 132 μm gesso layer. The guided modes that correspond to transmission coefficients lower than 10^{-2} are not considered in the optimization process. This gives a total of 16 modes to be used in the inversion process.

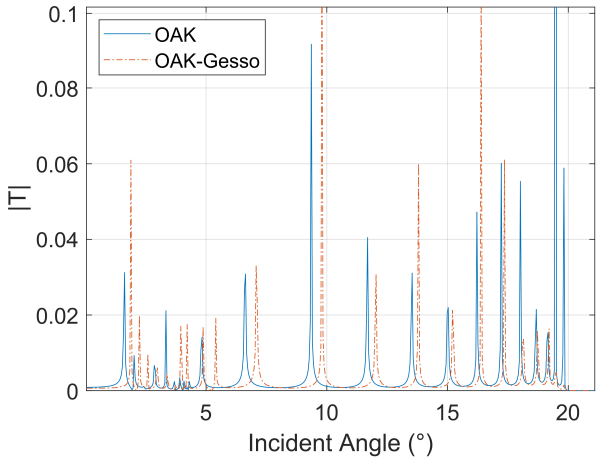

Fig. 11 Comparison between transmission coefficient of oak and oak-gesso bi-layer at 1 MHz.

One can observe the shift of the critical angles even when only a very thin layer of gesso covers the surface of the wood. The number of modes increases due to the presence of modes that mainly belong to the wood layer itself, but also to the gesso layer, and finally to the global structure (called coupling modes). The population size is set to have 100 individuals with the boundaries ranging from 0 to 5 GPa for the elastic constants, and from 500 to 800 kg/m^3 for the mass density when it is also considered unknown. Table 4 gives the mean values of the estimated elastic constants after 20 rounds and Table 5 shows the mean result when adding the mass density as an unknown.

	C_{11}(GPa)	C_{13}(GPa)	C_{55}(GPa)
Reference	4	1	1.5
Estimated	3.98 ± 0.03	0.94 ± 0.11	1.52 ± 0.04

Table 4 Elastic constants: reference and estimated for gesso at 1MHz.

	C_{11}(GPa)	C_{13}(GPa)	C_{55}(GPa)	$\rho(kg/m^3)$
Reference	4	1	1.5	800
Estimated	4.02 ± 0.20	0.87 ± 0.56	1.57 ± 0.20	799.77 ± 1.04

Table 5 Elastic constants and mass density: reference and estimated for gesso at 1MHz.

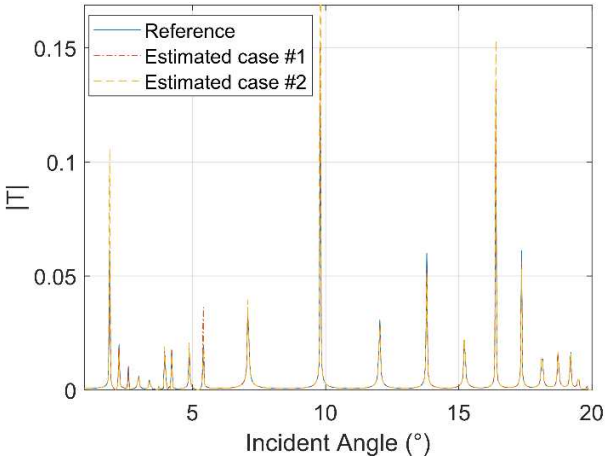

Fig. 12. Transmission coefficient of two layer oak-gesso structure, reference and estimated. Case 1 - three unknown elastic constants of gesso and Case 2 - three unknown elastic constants and unknown mass density of gesso.

As expected, the mean standard deviation in Table 5 is higher than the one of Table 4 since a new variable (mass density) must be determined by the Genetic Algorithm. However, this error can be decreased by increasing the size of population in GA, at the cost of increasing the computation time. Now looking at the mean estimated results in Table 4 and Table 5, it is possible to notice that the estimated values are close to the reference ones for C_{11} and C_{55}. The small thickness of gesso also suggests that the mass density is a parameter sensitive to optimization. However, C_{13} has a huge error compared to the reference values, even though the critical angles are very close to the estimated mean values and the reference ones as illustrated in Fig. 12 for the two cases. This occurs because the value of C_{13} does not impact the transmission coefficient of a very small layer as pointed out by Rokhlin and Wang in [27].

5. Conclusion

A numerical method to estimate elastic parameters of both isotropic and orthotropic plate samples, based on stiffness matrix model and a Genetic Algorithm has been developed. The optimization is based on an objective function that uses only the critical angles and the corresponding peak amplitudes - linked to guided modes in the sample - that appear in the transmission coefficient. The optimization is performed taking into account areas of the transmission coefficient that are located around the peaks (angles and amplitudes) of these modes, and not with the whole transmission coefficient, which avoids the need for a calibration of transducers. The recursive stiffness matrix method was chosen due to its stability when computing the transmission coefficient, particularly on thick samples. The optimization performed by a Genetic Algorithm implemented with wide boundaries provides

quite satisfactory estimations of unknown elastic parameters. However, numerical analysis reveals a higher estimation error when there are only two peaks in the transmission coefficient, which was the case for a 3mm acrylic plate at a frequency of 200 kHz. The elastic constants of acrylic, however, have been well estimated by increasing the frequency to 1MHz, which leads to an increase of the number of guided modes that are considered, from two at 200 kHz to five at 1 MHz. GA also appears to be a robust method since it demonstrates its capability of retrieving the right C_{55} value of the acrylic plate when it is considered as an unknown parameter: the estimation verifies the mathematical relationship with C_{11} and C_{13} As expected, the size of the GA population impacts the results of the estimation. With four elastic constants to determine in an oak sample, a population of 300 individuals was required for the optimization to reach satisfactory estimated parameters. The method also worked quite well on a bi-layer structure made of oak and a thin layer of gesso. The huge difference of thickness between these two layers did not prevent a good estimation of the elastic constants of Gesso, even when the mass density was considered as an unknown. The optimization was showed to be more sensitive to certain elastic constants than others, for both isotropic and anisotropic samples. In a bi-layer structure where gesso forms a very thin layer deposited on oak, a large sensitivity to mass density was also observed. The optimization using Simplex showed worse results than with the GA, even when the algorithm was used to estimate only two parameters. Future work will include using experimental transmission coefficients instead of simulated ones to test the robustness of the method and evaluate the impact of ultrasonic transducer diffraction. The method could also be applied to recover complex elastic moduli by considering the imaginary part of elastic constants, thus taking into account attenuation in samples.

Acknowledgments

This work was funded by a PhD grant from Université de Tours with logistical support of INSA Centre Val de Loire's campus in Blois.

Références

[1] G. Hübschen, I. Altpeter, R. Tschuncky and H.-G. Herrmann, Materials Characterization Using Nondestructive Evaluation (NDE) Methods, 2016, pp. 1-303.

[2] N. G. H. Meyendorf, P. B. Nagy and S. Rokhlin, Eds., Nondestructive Materials Characterization: With Applications to Aerospace Materials, Berlin Heidelberg: Springer-Verlag, 2004.

[3] A. M. Siddiolo, L. D'Acquisto, A. R. Maeva and R. G. Maev, «Wooden panel paintings investigation: An air-coupled ultrasonic imaging approach,» *IEEE Transactions on Ultrasonics, Ferroelectrics, and Frequency Control,* vol. 54, 2007.

[4] M. Kaczmarek, B. Piwakowski and R. Drelich, «Noncontact Ultrasonic Nondestructive Techniques: State of the Art and Their Use in Civil Engineering,» *Journal of Infrastructure Systems,* vol. 23, p. B4016003, May 2016.

[5] R. Green, «Non-contact ultrasonic techniques,» *Ultrasonics,* vol. 42, pp. 9-16, May 2004.

[6] G. J. Tserevelakis, P. Siozos, A. Papanikolaou, K. Melessanaki and G. Zacharakis, "Non-invasive photoacoustic detection of hidden underdrawings in paintings using air-coupled transducers," *Ultrasonics,* vol. 98, p. 94–98, September 2019.

[7] A. Zacharopoulos, K. Hatzigiannakis, P. Karamaoynas, V. M. Papadakis, M. Andrianakis, K. Melessanaki and X. Zabulis, "A method for the registration of spectral images of paintings and its evaluation," *Journal of Cultural Heritage,* vol. 29, p. 10–18, January 2018.

[8] D. E. Chimenti, «Review of air-coupled ultrasonic materials characterization,» *Ultrasonics,* vol. 54, pp. 1804-1816, 2014.

[9] H. Zhang, S. Sfarra, A. Osman, C. Ibarra-Castanedo and X. P. V. Maldague, «Using through-transmission mid-wave infrared vision and air-coupled ultrasound for artwork inspection: a case study on mock-ups of Portrait of the Painter's Mother,» *Insight - Non-Destructive Testing and Condition Monitoring,* vol. 62, p. 123–128, March 2020.

[10] B. Hosten, D. A. Hutchins and D. W. Schindel, «Air-Coupled Ultrasonic Bulk Waves to Measure Elastic Constants in Composite Materials,» chez *Review of Progress in Quantitative Nondestructive Evaluation: Volume 15A*, D. O. Thompson et D. E. Chimenti, Éds., Boston, MA: Springer US, 1996, p. 1075–1082.

[11] M. Castaings and B. Hosten, «Air-coupled measurement of plane wave, ultrasonic plate transmission for characterising anisotropic, viscoelastic materials,» *Ultrasonics,* vol. 38, pp. 781-786, 2000.

[12] B. Hosten, M. Castaings, H. Tretout and H. Voillaume, «Identification of composite materials elastic moduli from Lamb wave velocities measured with single sided, contactless ultrasonic method,» *AIP Conference Proceedings,* vol. 557, pp. 1023-1030, April 2001.

[13] S. Dahmen, H. Ketata, M. H. B. Ghozlen and B. Hosten, «Elastic constants measurement of anisotropic Olivier wood plates using air-coupled transducers generated Lamb wave and ultrasonic bulk wave,» *Ultrasonics,* vol. 50, pp. 502-507, 2010.

[14] H. Zhang and D. Chimenti, «Air-Coupled Transmission Coefficient Reconstruction Using a 3-D Complex-Transducer-Point Voltage Model,» *Journal of Nondestructive Evaluation,* vol. 22, pp. 23-37, March 2003.

[15] S. I. Rokhlin and L. Wang, «Stable recursive algorithm for elastic wave propagation in layered anisotropic media: Stiffness matrix method,» *The Journal of the Acoustical Society of America,* vol. 112, p. 822–834, September 2002.

[16] J. Vishnuvardhan, C. V. Krishnamurthy and K. Balasubramaniam, «Genetic algorithm based reconstruction of the elastic moduli of orthotropic plates using an ultrasonic guided wave single-transmitter-multiple-receiver SHM array,» *Smart Materials and Structures,* vol. 16, p. 1639–1650, August 2007.

[17] A. A. Eremin, E. V. Glushkov, N. V. Glushkova and R. Lammering, «Evaluation of effective elastic properties of layered composite fiber-reinforced plastic plates by piezoelectrically induced guided waves and laser Doppler vibrometry,» *Composite Structures,* vol. 125, pp. 449-458, 2015.

[18] N. Bochud, J. Laurent, F. Bruno, D. Royer and C. Prada, «Towards real-time assessment of anisotropic plate properties using elastic guided waves,» *The Journal of the Acoustical Society of America,* vol. 143, pp. 1138-1147, 2018.

[19] L. Zhu, X. Duan and Z. Yu, «On the Identification of Elastic Moduli of In-Service Rail by Ultrasonic Guided Waves,» *Sensors,* vol. 20, 2020.

[20] L. M. Brekhovskikh et O. a. Godin, Acoustics of layered media I : plane and quasi-plane waves, 1990.

[21] S. Dodd, J. Cunningham, A. Miles, S. Gheduzzi and V. Humphrey, «Ultrasonic propagation in cortical bone mimics,» *Physics in medicine and biology,* vol. 51, pp. 4635-47, October 2006.

[22] M. R. Karim, A. K. Mal and Y. Bar-Cohen, «Inversion of leaky Lamb wave data by simplex algorithm,» *The Journal of the Acoustical Society of America,* vol. 88, p. 482–491, July 1990.

[23] J. Lagarias, J. Reeds, M. Wright and P. Wright, «Convergence Properties of the Nelder–Mead Simplex Method in Low Dimensions,» *SIAM Journal on Optimization,* vol. 9, p. 112–147, December 1998.

[24] S. Kumar, «A CAS Approach to Handle the Anisotropic Hooke's Law for Cancellous Bone and Wood,» *Chinese Journal of Engineering,* vol. 2014, pp. 1-28, March 2014.

[25] J. Dong, A. Locquet, M. Melis and D. Citrin, «Global mapping of stratigraphy of an old-master painting using sparsity-based terahertz reflectometry,» *Scientific Reports,* vol. 7, p. 15098, November 2017.

[26] B. Rachwał, L. Bratasz, L. Krzemien, M. Łukomski and R. Kozlowski, «Fatigue Damage of the Gesso Layer in Panel Paintings Subjected to Changing Climate Conditions,» *Strain,* vol. 48, December 2012.

[27] S. I. Rokhlin and W. Wang, «Measurements of elastic constants of very thin anisotropic plates,» *The Journal of the Acoustical Society of America,* vol. 94, pp. 2721-2730, 1993.

470

471

472

473